

# **FINAL PROGRESS REPORT**

## **Application of Automatic Control to A Single Flash Desalination Unit**

(Project number 3/419)

**Prepared by: Dr. Emad Ali (Principal Investigator)**

Dr. Kahlid Alhumaizi (Co Investigator)

Dr. Abdulhamid Ajbar (Co Investigator)

Chemical Engineering Department

King Saud University

## **Acknowledgment**

The investigators are very grateful to SABIC for supporting this project financially under the program for funding short-term academic research projects. The investigators would also like to thank the general directorate of research center at the college of engineering for their support, continuous follow up and patience throughout the project duration. We would like to emphasize the benefit and advantage of this program, which enables the scientist and scholars to manifest their research ideas into realistic application.

The investigators would like also to thank the chemical engineering department for providing lab facilities such as space and utilities in addition to laboratory materials and accessories.

# Table of Contents

| <u>Content</u>  | <u>Page</u> |
|---|-------------|
| Summary   | 1           |
| 1. Introduction   | 2           |
| 2. Literature survey  | 3           |
| 3. MSF process  | 5           |
| 4. MSF plants control loops                                   | 7           |
| 5. Physical process flow-sheet and setup                      | 9           |
| 6. Mathematical model   | 15          |
| 7. Implementation issues                                      | 17          |
| 8. Experimental tests   | 20          |
| 8.1 Open-loop runs  | 20          |
| 8.1.1 Temperature startup at fixed pressure and heat load     | 20          |
| 8.1.2 Temperature startup at fixed pressure and brine flow    | 27          |
| 8.1.3 Temperature startup at fixed brine flow and heat load   | 35          |
| 8.2 Closed-loop runs  | 36          |
| 8.2.1 Temperature startup with on-off controlled flow rate    | 36          |
| 8.2.2 Temperature startup with on-off controlled heater power | 36          |
| 8.2.3 Temperature startup with PI controlled heater power     | 37          |
| Conclusion  | 44          |
| Nomenclature  | 46          |
| References  | 47          |

## Summary

A comprehensive design and installation of an experimental set up is achieved in this work. The set up resembles a single-stage flash desalination unit, which is a major unit in the multi-stage flash desalination processes running in Saudi Arabia. The process consists of a brine heater and a flash unit with a condenser. The brine heater is used to heat the brine inlet to the flash unit up to a desired temperature using an electrical heater. The brine flashes inside the flash unit due to vacuum and the condenser is used to condense the vapor produced from flashing. The condensed vapor is drawn out as the distillate product.

Extensive open-loop dynamic tests were carried out to understand and analyze the process dynamic. The dynamic analysis is also useful to design a suitable control strategy for such process. Simple closed-loop tests were carried out to test process behavior under control. The main objective of the control investigation is to design a good control system for this process, which in turn improves its operation. The investigation revealed the existence of a potential for enhancing the process operation through good control implementation. Further control analysis and studies require more time. In addition, some technical problems, which are mentioned inside the report, should be addressed in order to conduct further research work. A theoretical model for the process is developed. However, the model was not validated for time shortage and the technical problems mentioned earlier.

The experimental set up as it stands is an excellent contribution to the University laboratory, which can be employed to educate and train both undergraduate and graduate students at the chemical engineering department. In addition, the investigators learned and gained considerable experience from such project.

## 1. Introduction

It is well known that fresh water is not available in every part around the world. Moreover, some of the available water resources require special form of treatment. This situation created water shortages in 88 developing nations that contain almost half of the world population [1]. Even in countries where water supplies are plentiful, water shortages start developing due to long period of erratic rainfall. Consequently Governments of such countries started to impose restrict water usage. As population and industry increases, water demands increases. As a result water supplies cannot meet the demands of urban and industrial development and the associated changes in the lifestyle. The current water shortage forced many countries, industrialized or developing, to look for other sources of fresh water. One solution is to desalinate seawater. Two major procedures are used for seawater desalination, Reverse Osmosis (RO) and Multi Stage Flash (MSF) desalination. Multi stage flash desalination is the widely used technology especially in the Gulf countries. The limited use of RO in the Gulf area is attributed to its harsh weather, which RO membrane can not handle. It is reported that world desalination capacity at the end of 1997 is above  $22.8 \times 10^6$  m<sup>3</sup>/day, and the number of operating units is more than 12,506 [2] found over 120 countries. However, the Gulf countries account for more than half of the total world production [3].

MSF desalination became the main source of fresh water for domestic, industrial and agricultural consumption. In fact, MSF water production amounts to 53% of the total worldwide production, while RO amounts to about 36% [3]. Contracts for new plants is also in proportion to the world production where 58% of the new plant are based on MSF process and 25% on the RO process. MSF process belongs to the thermal separation technique including two main processes, which are evaporation followed by condensation. The major advantage of MSF is that evaporation occurs due to pressure vacuum in the bulk fluid away from the surface of hot tubes. Therefore, loss of efficiency and material due to scale and corrosion is avoided. The paramount importance of desalination in producing potable water, draw the attention of many engineers and researchers to enhance the operation of such plants in the most efficient manner possible.

## 2. Literature Survey

The basic fundamentals of desalination in general and MSF technology in particular are covered in some textbooks and others [4,5,6]. The pioneering work on MSF desalination is due to Silver [7,8]. Several research efforts were devoted for the modeling and simulation of MSF plants. Steady state modeling is conducted by Beamer and Wilde [9], Hayakawa *et. al.* [10], Helal *et. al.* [11] and Al-Mutaz and Soliman [12]. On the other hand, dynamic modeling is investigated by many others such as Glueck and Bradshaw [13], Delene and Ball [14], Rimawi *et. al.* [15], Reddy *et. al.* [16] and Hussain *et. al.* [17,18]. More recently, Thomas *et. al.* [19] developed a steady state and dynamic model for MSF desalination plant and validated their model with real time data. Similarly, many researchers studied the empirical modeling of MSF plants using real time process data [20-22]. On the same line, Neural Network algorithm is also adopted for dynamic modeling of MSF plants [23,24].

Most of the MSF plants are controlled by conventional PID control algorithms and lack robust stability [25]. Early efforts concerned with control design and implementation for MSF plants exist. For example, supervisory controller based on mathematical correlation is investigated [26-28]. Despite the drastic advancement in the control theory and technology, the state of MSF control systems still far behind these enhancements. Nevertheless, MSF plants have the potential for modern control implementation. Modern control algorithms can help in improving the plant operation and safety, reducing the shut down frequency caused by severe load upsets, providing smooth transition from one operating condition to another, and optimizing the consumption of resources and energy. This potential motivated researchers towards investigating the automation, optimization and control of MSF plants. As mentioned earlier, developing empirical models that are suitable for advanced control application is investigated [20-23]. Krause and Hassan [29] addressed the online optimization of MSF plants using existing mathematical models for MSF plants. Loop selecting and tuning of MSF controllers is studied by El-Saie and Hafez [30].

The current status of the control systems employed in MSF plants is analyzed by Al-Gobaisi *et. al.* [31-33]. The latter pointed that implementation of modern control techniques to MSF plants have not been addressed thoroughly. Similarly,

Ismail [34] reviewed the control strategies implemented in MSF plants and pointed the existence of promising results in the cultivation of modern control techniques to such plants. The possibility of applying Fuzzy control algorithms to MSF plant have been also addressed by Olafsson [24], Akbarzadeh and Kumbala [35] and Kumbala and Akbarzadeh [36], Akbarzadeh *et. al.* [37] and Ismail [38]. Other advanced control approaches such as linear Model Predictive Control is also studied by Maniar and Deshpande [39]. Nonlinear Model Predictive Control has been proposed and studied by Ali *et. al.* [40,41]. However, Most of the reported efforts are limited to simulation investigation. Further practical studies and real time testing of advanced control algorithms is necessary for the enhancement of MSF automation and control.

### **3. MSF Process Description**

In a typical MSF plant as shown in Figure 1, we can distinguish between three basic sections: heat rejection section, heat recovery section and the brine heater. Complying with the convention used in counting the stage number of MSF, counting starts from the most left stage, i.e. the first stage is the stage next to the brine heater. The last stage is the stage into which the seawater is fed. The recovery and reject sections consist of a series of stages. Each stage has a flash chamber and a condenser. In the flashing chamber, vapor is flashed off and rises up to a demister, which intercepts brine droplets entrained in the flashing vapor. A distillate tray, located under the condenser tube, collects the condensate.

The salty seawater is pumped to the last stage through the condenser tubes. On leaving the first (warmest) rejection stage the feed stream is split into two parts, reject sea water which passes back to the sea and a make up stream, which is then combined with the recycle stream. The combined stream passes through a series of heat exchangers, its temperature rising as it proceeds towards the heat input section of the plant. Passing through the brine heater the brine temperature is raised from the feed temperature at the inlet of the brine heater to a maximum value, approximately equal to the saturation temperature at the system pressure. The brine then enters the first heat recovery stage through an orifice thus reducing the pressure. As the brine was already at its saturation temperature for a higher pressure it will become superheated and flashes to give off water vapor. The vapor then passes through a wire mesh (demister) to remove any entrainment brine droplets and onto a heat exchanger, where the vapor is condensed and drips into a distillate tray. The process is then repeated all the way through the plant as both brine and distillate enter the next stage which is at a lower pressure. The concentrated brine is divided into two parts as it leaves the plant; a blow-down, which is pumped back to the sea and a recycle stream, which returns to mix with the make up steam.

The flow of brine in the flashing chamber is caused by the pressure drop and the liquid level is maintained by adjusting the orifice height in each chamber. However, severe disturbance in the re-circulating brine flow may cause instability in the brine level. Therefore, the interstage orifice design is a very essential part of any

MSF unit. It should maintain low brine level to avoid vapor blow-through. The capacity of MSF plants is driven by the top brine temperature (TBT) entering the first stage. TBT, and consequently the MSF capacity, is limited by the capacity and performance of the brine heater. Different MSF configurations are available and future outlook regarding the MSF design modification is presented in the literature [1].

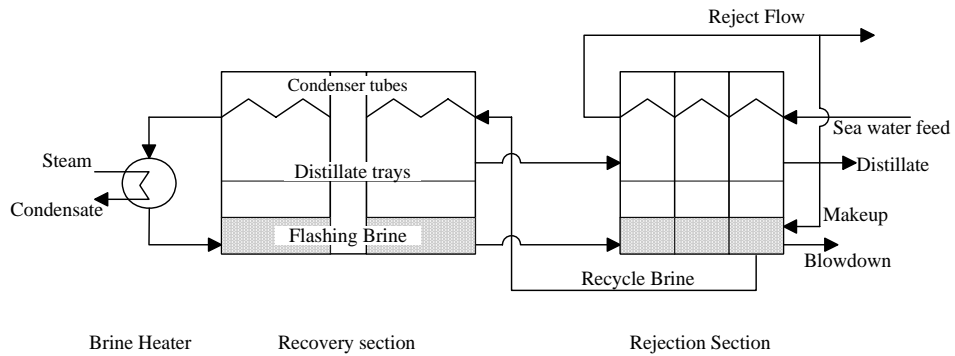


**Figure 1: Schematic of MSF Plant**

#### 4. The MSF plant Control loops

Like any chemical process, the plant is operated and inventory is maintained by several basic control loops. Detail discussion of the general MSF control loops is given by Al-Gobaisi *et. al.* [30]. In the following we present a brief summary of some of the traditional MSF control loops.

- *Makeup flow control*: The makeup flow is controlled using basic ratio controller. The purpose is to maintain constant brine concentration. The set point for the Makeup flow is the sum of the distillate and Blow down flow rates.
- *Brine level control*: The brine level in the last stage is controlled via manipulating the set point of the blow down flow rate. This will also affects the level in the preceding stages. The main disturbances to this control loop are the brine recycle flow rate and the flash temperature range.
- *Distillate level control*: The distillate level in the last stage is controlled via manipulating the set point of the outlet flow rate. This will also affects the level in the preceding stages.
- *Seawater flow control*: The seawater feed is controlled by manipulating the pump speed. This will affects the heat transfer in the reject section.
- *Seawater feed temperature control*: The feed temperature is controlled by manipulating the flow of cooling water circulated around the reject section. This affects the heat transfer in the reject section. It also affects the makeup temperature and consequently the temperature of the brine re-circulating flow.
- *Low Pressure steam temperature and pressure control*: The temperature of the steam is controlled by manipulating the water flow rate in the de-superheater. The steam pressure is controlled by manipulating a pressure-reducing valve.
- *Brine heater condensate level control*: The condensate level in the brine heater is controlled by manipulating the flow of the discharge. This affects the heat transfer in the brine heater and consequently the efficiency of the brine heater.
- *Brine re-circulating flow control*: The brine recycle flow is controlled by manipulating its pumping power. This directly affects the brine level in the flashing chamber and the steam consumption for a fixed TBT. High recycle

flow result in less flashing efficiency, less residence time and higher brine level.

- *TBT control*: TBT is controlled by manipulating the steam flow rate. This affects directly the production capacity. The main disturbances to this control loop is the steam temperature/pressure, brine recycle flow rate and the brine recycle temperature.

Throughout the world, all of the above control loops are handled by standard PID-type control algorithms. The loops are configured in a multi loop SISO structure. However, the MSF plant is highly interactive multivariable process. Therefore, the SISO PID scheme may lack robustness and may perform poorly. In addition, as mentioned earlier, poor level control may lead to instability in form of blow through or flooding, which may cause loss of efficiency or even shut down of the process. Moreover, MSF is highly heat intensive and a potential exist for energy optimization. The performance ratio, the ratio of distillate produced per unit mass of steam consumed, is well known to be normally around 8. There have been many studies concerned with improving the performance ratio through novel design procedure [1]. However, good control system can also help improving such ratio or at least maintain it during disturbance [39]. The latter is very common to all MSF plants and the current primitive control system has poor suppression for such disturbances. According to the problems discussed above, MSF needs more reliable and robust control system that can take account of all possible internal and external disturbances. Moreover, the proposed control system should be able to minimize the power consumption.

For the purpose of improving the MSF control design, Sarkar *et. al.* [42] has designed a laboratory scale single stage flash desalination unit. The unit is designed to test he application of advanced control systems on such lab-scale unit. The objective of this research is similar in concept to the work of Sakar *et. al.* A laboratory scale single stage flash desalination unit is designed and assembled for the purpose of extensive testing proposed control systems. The testing will consider the reliability, efficiency and robustness of the proposed modern control systems. The results of such testing should further assess the enhancement of controllers for desalination plants.

## 5. Physical process flow-sheet and setup

The flow sheet of the process (experimental setup) is shown in figure [2]. The setup is build and installed in the chemical engineering laboratory. The electronic parts (sensors) of the setup are listed in Table [1]. These are provided via international vendors. As shown in Figure [2] there is a main cylindrical vessel, which represents the flash chamber. It is made of glass that stands maximum temperature of 100 °C and has a capacity of 5~10 Liters. The brine storage tank is filled with tap water and has a capacity of 50 Liters. Brine flows out of the tank by means of centrifugal pump and fed into the condenser coil, which is made of brass. After getting heated by the condensing vapor, the brine is fed into external heater. The brine stream is continuously heated and fed to the flash chamber. At the flash chamber, the hot brine vaporized due to vacuum. The concentrated brine is withdrawn out of the chamber using a pump. The pressure inside the chamber is maintained via a vacuum pump. The hot vapor travels up through the perforated plate until it reaches the condenser coil. At the condenser, the vapor gives up its latent heat and turn into condensate, which drips back to a collector plate. The distilled water is then withdrawn via a centrifugal pump.

The external heater is a glass vessel of 20-liter capacity. The heater is filled with fixed amount of water. The water is heated by two electrical heaters, each of which has a power of 1000 Watt. The hot water is used to heat up the circulating brine. The latter flows inside a brass coil immersed inside the hot water. In addition to the external heater, a quench tank is used to cool down the blow down. The objective of the cooler is to keep the temperature of the brine outlet below 40 °C. This is necessary for proper operation of the conductivity meter, which operates at maximum ambient temperature of 40 °C.

Several electronic measuring devices are located at different points to measure the process variables. The chamber pressure is measured via a pressure transducer mounted at the top of the vessel. Type-k thermocouple probes are used to measure the temperature of the brine feed to the condenser, condenser outlet, brine feed to the flash chamber, brine inside the chamber. Similarly, a thermocouple is used to measure the heater temperature. Both float flow meter and electrical flow sensor are used to

measure the flow rate of circulating brine feed, brine leaving the chamber (blow down) and the distillate. Bench-top digital conductivity meters are used to measure the brine concentration of the brine feed and blow down.

Regular needle valves are used to regulate the flow rates of the distillate and the blow down. A solenoid control valve is used to regulate the brine feed flow rate. All measured signals are transmitted to the personal computer through data acquisition system. The control valve receives electrical commands from the computer through the data acquisition to actuate the brine flow rate.

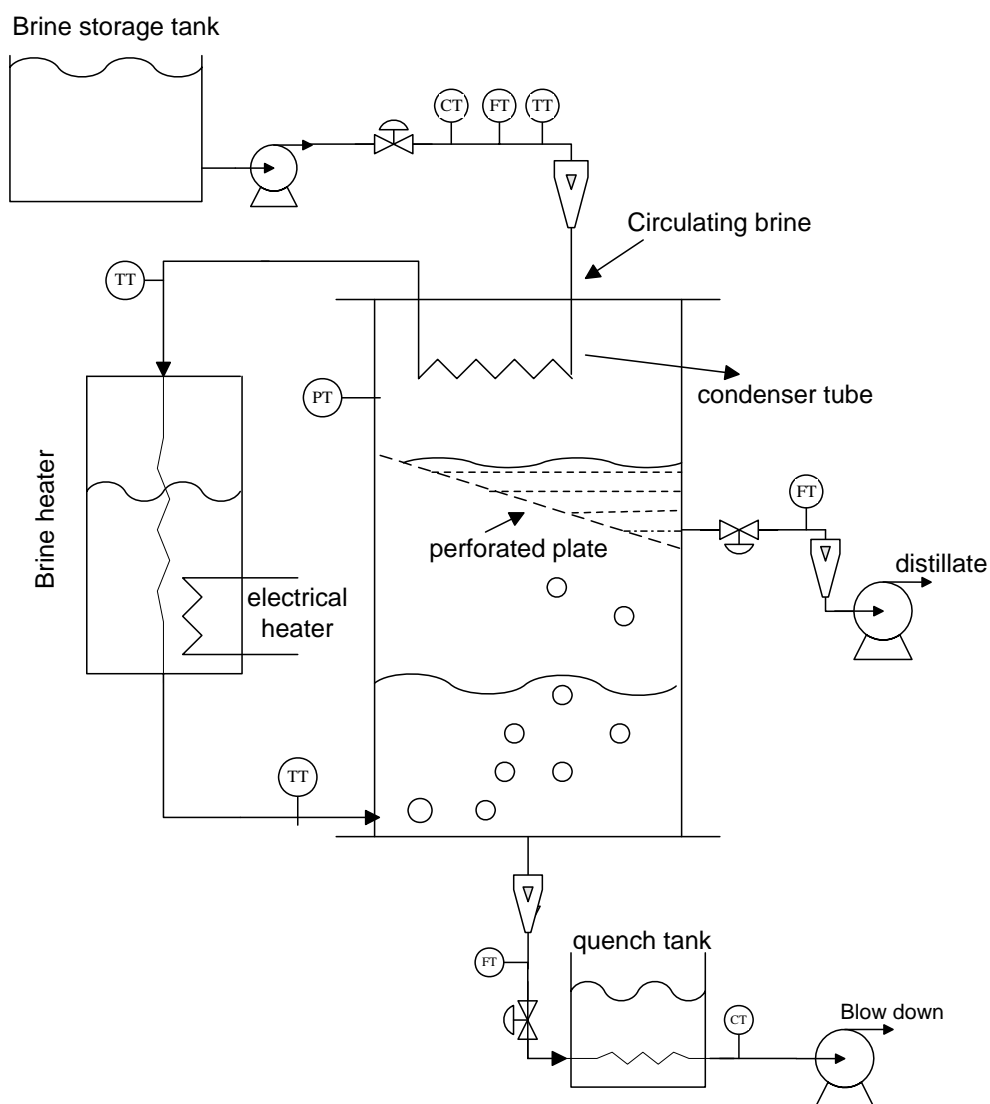


Figure 2: Schematic of the single flash desalination unit

A multi channel data acquisition system is used as interface between the various process sensors and the computer. The main function of the data acquisition is to process all measured data and transfer them between the computer and the process actuators back and forth. A 330 MHz Pentium II personal computer is used in this experiment. The personal computer function is data logging, processing, analysis and manipulation. The computer is also used to synchronically calculate new control actions. The new actions are sent via the data acquisition system to the process actuators. In this case. The sensors, data acquisition system, personal computer and control valves comprise the basic elements of the process feedback control loop

**Table 1: Equipment list**

| <i>Equipment</i>            | <i>Quantity</i> | <i>Specification</i> |
|-----------------------------|-----------------|----------------------|
| Brine Tank                  | 1               | 50 G                 |
| Main vessel                 | 1               | 30 L                 |
| Electrical heater           | 1               | 1500W, 115V          |
| Manual valve (Needle)       | 4               | ~2.8 LPM, SS         |
| Solenoid valve (on/off)     | 1               | Cv=1.92              |
| Control valve               | 3               | ~3 LPM, Cv=0.24      |
| Control module + Cord       | 3               |                      |
| Flow meter                  | 4               | 0.2~ 3 LPM           |
| Turbine Flow Sensor         | 2               | 16-400 GPH           |
| Regular Flow sensor         | 2               | 0.1~2 LPM            |
| Power supply                | 2               | 120 V                |
| Pump                        | 3               | 0~2.3 LPM            |
| Pressure transmitter        | 1               | ~30psig              |
| Level sensor                | 1               | SS                   |
| Level controller switch     | 1               |                      |
| Level transmitter accessory | 1               | Ultrasonic           |
| Temperature Sensor          | 4               | ~482°C, Type K       |
| Conductivity meter          | 2               | 2~2000 ms            |
| Data acquisition            | 1               | Analog 16IN/2OUT     |
| Terminal Panel              | 1               | Digital 8 IO         |
| Personal Computer           | 1               |                      |

## 6. Process model

The following represent the dynamic model for the single-stage flash desalination unit based on constant physical properties. In addition, no boiling point rise is considered, which means that the vapor condensate at the brine temperature inside the flash chamber. Similarly, no thermal loss is considered, thus, the total condensate equals the vapor produced by flashing.

*Energy balance for the brine heater:*

Shell side:

$$V\rho C_p \frac{dT}{dt} = Q - UA(T - 0.5(T_{B0} + T_{Bi})) - h(T - Ta)$$

Tube side:

$$m_B C_p \frac{dT_{B0}}{dt} = B_r C_p (T_{Bi} - T_{B0}) + UA(T - 0.5(T_{B0} + T_{Bi}))$$

*Mass balance for the brine in the flash chamber:*

$$\frac{dm}{dt} = B_r - B_D - V_d$$

*Salt balance in the flash chamber:*

$$m \frac{dx}{dt} = B_r x_i - B_D x$$

*Energy balance in the flash chamber:*

$$m C_p \frac{dT_{B1}}{dt} = B_r C_p (T_{B0} - T_{ref}) - B_D C_p (T_{B1} - T_{ref}) - V_d \lambda$$

*Energy balance around the condenser tube:*

$$m_c C_p \frac{dT_c}{dt} = B_r C_p (T_{ci} - T_c) + V_d \lambda_s$$

*Mass balance around the distillate tray:*

$$W_D = V_d$$

## **7. Implementation issues**

### **7.1 Fluid circulation**

It is mentioned in the earlier section that the brine flows into the condenser then heater tank and finally into the flash chamber. Relying on static head is not enough to create sufficient flow rate. For this reason miniature Gear pumps were installed to maintain fixed flow rates. In this case, the small pumps can deliver steady flow rate in the range of 0-1000 cc/min. Similarly, the produced distillate and the blow down can not be withdrawn easily due to their small static head and moreover due to the vacuum inside the flash chamber. Therefore, miniature Gear pumps were installed to maintain fixed flow rates

### **7.2 Instrument calibration**

The basic instrument used in the experiment transmits the measured variable in terms of voltage signals. The signal range is 0-5V. This is the common communication media between the data acquisition card and digital computers. For more scientific application, it is more useful to convert these signals into suitable engineering units. In this experiment, the fluid flow measurement, temperature measurement and the salt concentration measurement should be converted (calibrated) into their corresponding units.

#### **7.2.1 Flow sensor calibration:**

First the fluid flow measurement is calibrated. This was achieved through recording the voltage reading produced by the flow sensor and the corresponding flow rate reading provided by the regular flow meter. Different readings were taken to cover the available span for the fluid flow of 100-2000 cc/min. This procedure is repeated for the acid stream.

Since the flow-volt readings seem to be linear, a linear fitting correlation is proposed as follows:

$$F = b + a * V$$

Where  $F$  is the flow rate and  $V$  is the voltage reading.  $a$  and  $b$  are fitting parameters. Fitting the above correlation to the collected data, using Sigma plot software, suggests the following values for the parameter:

$$a = 474.2, \quad b = 15.8$$

The original data and the fitted correlation are plotted together for comparison purposes as shown in Figure 3. It is clear that the fitted correlation is in excellent agreement with the process data. Note that, the result is identical for both flow rates, i.e. alkaline and base. The obtained correlation is then inserted in the workbench software so that the transmitted signal is converted directly into flow units.

### **7.2.2 Thermocouple calibration**

The temperature is measured using type-K thermocouple. The thermocouples are calibrated using a temperature calibrator. The calibrator is an electronic device available at the chemical engineering laboratory.

### **7.2.3 Salt concentration calibration:**

The dissolved salt conductivity is measured by a bench-top conductivity meter. The measured conductivity of the salt should be converted into concentration units of gm/L. Different sample of brine solution with known concentration are used to calibrate the conductivity meter. The conductivity of each sample is measured and a plot for the measured conductivity versus the salt concentration is shown in Figure 4. Clearly the concentration-conductivity relation is linear with a slope of 0.5. Therefore, The salt concentration can be inferred directly from the measured conductivity according to:

$$C \text{ (gm/L)} = 0.5G \text{ (ms/cm)}$$

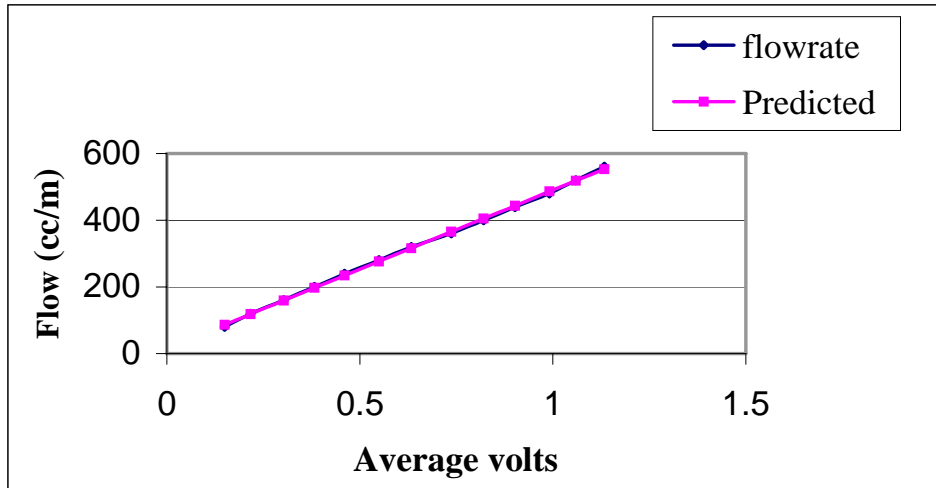


**Figure 3: Experimental data for calibrating the flow sensors**

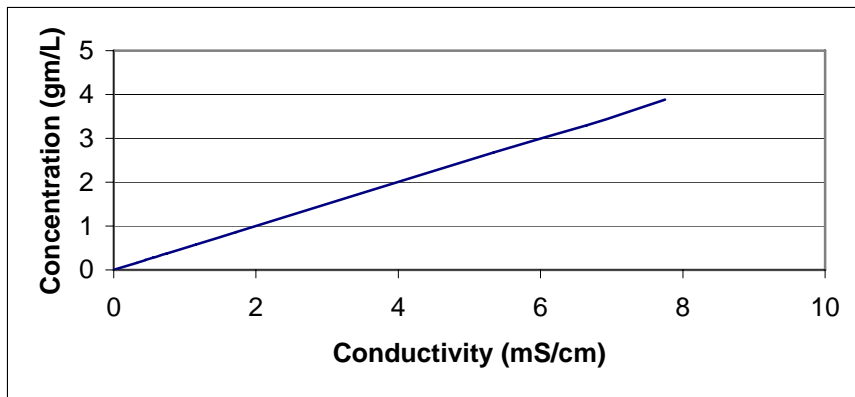


**Figure 4: Experimental data for calibrating the conductivity meter**

## **8. Experimental tests**

### **8.1 Open-loop runs**

Preliminary runs were conducted to debug the instruments and test the operation of the process. Afterwards, open loop testes were carried out to determine the steady state operating condition of the process. The water level in the heater is maintained via an overflow pipe. The liquid level inside the flash chamber is maintained by manual adjustment of the inlet flow (circulating brine) and the outlet flow (blow down). After maintaining the process inventory, i.e. flow rates and levels, it remains to determine the steady state operating temperature of the water inside the brine heater and of the brine inside the flash chamber. This will be done without production of distillate. The objective is to study the thermal behavior of the heater without the interference of external disturbances. The following step is to determine the steady state distillate production.

#### **8.1.1 Temperature start-up at fixed pressure and heat load:**

In the following tests, the experiment is run at fixed pressure for the flashing chamber of 1 atmosphere. The heater load is also set to its maximum. The pressure is kept constant at 1 atmosphere intentionally to avoid evaporation because our objective is simply to determine the maximum steady state temperature for the process with maximum heating load.

The brine heater has a fixed energy source of 2000 watt equivalent to 2000 J/s. Therefore, there exists a steady state temperature for the water inside the heater and for the brine leaving the heater tube. The steady state value depends on the flow of the circulating brine. Figure 5 shows the temperature response to start up operation. The process starts from room temperature and the electric heater is turned on at maximum capacity. The circulating brine flow is set to a fixed value of 540 cc/min. The system is allowed to reach steady state freely.

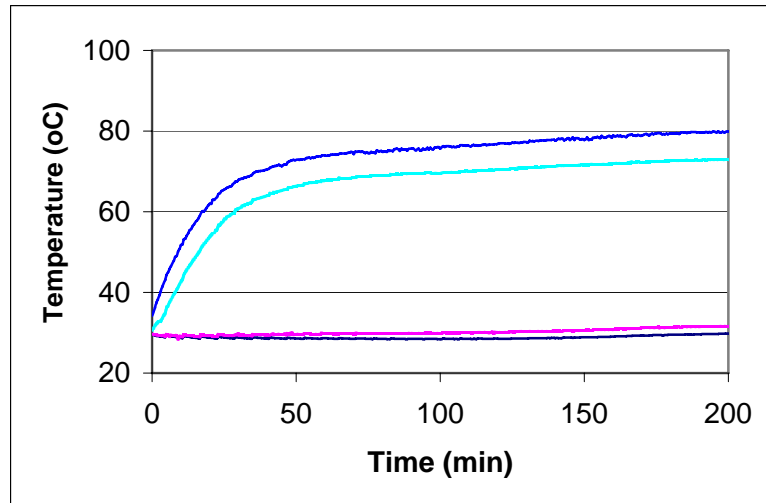


**Figure 5: Temperature response to start up from room temperature using  $F = 540$  cc/min.**

The test is carried out over 3 hours with sampling time of 0.5 minute. As shown by the figure, the heater temperature reaches 80 °C where the brine temperature reaches 70 °C at steady state. The figure shows the brine temperature at the inlet and outlet of the condenser tubes. Both temperatures were almost constant around the their initial values. This is because no evaporation and condensation occurs. No evaporation occurs because the brine temperature is below the boiling point at 1 atm. The above test is repeated using fixed flow rate of 400 cc/min. Figure 6 illustrates the new steady state starting from room temperature. In this case, both process temperatures reach higher values. Specifically, the heating water approaches 87 °C and the brine temperature reaches 77 °C. Similarly, Figure 7 shows the temperature response for startup from room temperature using brine flow rate fixed at 352 cc/min. This time, the heated water temperature reaches 93 °C and the brine 79 °C. Obviously, the steady state temperature increases with reduction of circulating brine, which is fundamentally sound. Figure 8 depicts the same open-loop test, but with brine flow rate fixed at 260 cc/min. In this case, the heater temperature increased substantially because the brine flow rate is small. The experiment is terminated as the heater temperature approached 100 °C to avoid local boiling and damages of the sensitive sensors. The dynamic of the heater is govern by the following model equations:

*Energy balance for the water mass:*

$$V\rho C_p \frac{dT}{dt} = Q - UA(T - 0.5(T_{Bo} + T_{Bi})) - h(T - T_a)$$

*Energy balance for the circulating brine:*

$$M_B C_p \frac{dT_B}{dt} = B_r \rho C_p (T_{Bi} - T_B) - UA[T - 0.5(T_{Bo} + T_{Bi})]$$

where  $T$  is the temperature of the heated water,  $T_{Bo}$  is the brine temperature at the outlet and  $T_{Bi}$  is the brine temperature at the inlet.  $V$  is the water volume inside the heater,  $M_B$  is the brine mass holdup inside the tube and  $B_r$  is the volumetric flow rate of the brine.  $Q$  is the inlet heat produced by the electrical heater and equals 2000 J/s when operating at maximum throughput. The only unknown in the above model is the term  $UA$ , which represents the overall heat transfer coefficient multiplied by the heat transfer area. The unknown parameter can be identified from the experimental data using the steady state version of the above equation. Figure 9 shows the value of the unknown parameter as a function of the brine flow rate. Similarly, Figure 9a shows the steady state gain relating the brine temperature to the brine flow rate. As clear from figure 9, the parameter  $UA$  increases with brine flow rate. The relation is almost linear except at an intermediate value, which might be a result of human or experimental error. On the other hand, the  $T_{Bo}$ - $B_r$  gain is negative and its magnitude decrease with increasing flow rate.

The effect of a single step test in the brine flow rate is shown in the previous figures. The next two figures show the process temperature response to consecutive step changes in the brine flow rate. For example, Figure 10 depicts the temperature response to step change in the brine flow rate from 0 to 260 cc/min starting from room temperature. The heater is also turned on maximum load at the same time. At time equals 80 minutes, with the heater still at maximum load, the brine flow rate is stepped again to 480 c/min. The step changes in the brine flow rate are shown in Figure 10a. Clearly, the process temperature increased in the beginning. However,

after the brine flow rate is increased, the temperature obviously dropped to a new steady state value. This behavior is in agreement with the negative gain for the  $T_B$ - $F$  variables. Some temperature increase is observed in the 160-200 minute interval of the experiment life. This is due to the voluntarily decrease in the brine flow rate as shown in figure 10a. The flow rate was adjusted later manually.

Figure 11 depicts the temperature response to step change in the brine flow rate from 0 to 600 cc/min starting from room temperature. The heater is also turned on maximum load at the same time. At time equals 100 minutes, with the heater still at maximum load, the brine flow rate is stepped again to 400 c/min. The step changes in the brine flow rate are shown in Figure 11a. It is noted that in the second step the heated water does not reach a steady state although more than 2 hrs was elapsed. This is because the brine temperature at the heater inlet is increasing in a ramp fashion. The brine temperature at the heater inlet, which is in fact the temperature for the brine coming out of the condenser tube, increases because of the condensing vapor at the condenser tube. Although the condensation is minor, but it effected the brine temperature flowing in the condenser tube.

The above open-loop tests was useful in understanding the thermal behavior of the process when operating at maximum heat load and without vacuum, i.e. without evaporation. In addition, important process parameter, i.e.  $UA$ , is identified and the dynamic characteristics for the  $T_B$ - $F$  pair, such as steady state gain and time constant, are determined. However, some operational difficult exit. For example, the water level in the flashing chamber can not be maintained at steady value. Even if the inlet and outlet flow of the flash chamber is kept constant, water level can not stabilized. This happens for two reasons:

1. Precision of the standard rotameters used to regulate the flow rates. Minute error in the rotameter readings makes its effect on the level when long time is elapsed.
2. Sudden voluntary changes in the flow rates. This might occur due to air bubbles entrapped in the flow lines, changes in the temperature, or changes in the fluid static head. The later applies for the outlet flow only.

It should be noted, however, that changes in the water level inside the flash chamber have no effect on the thermal behavior of the brine heater. Exception is for the temperature readings inside the chamber, which might get corrupted if the level goes below the tip of the thermocouple. Another disadvantage of the level fluctuation is that continuous monitoring of the level is necessary to avoid drainage of the flash chamber.

The sudden change in the flow rate as mentioned in item 2 above has another impact on the process operation. Continuous changes in the circulating brine flow prevent the heater from reaching steady state. This situation is clear in Figure 10.

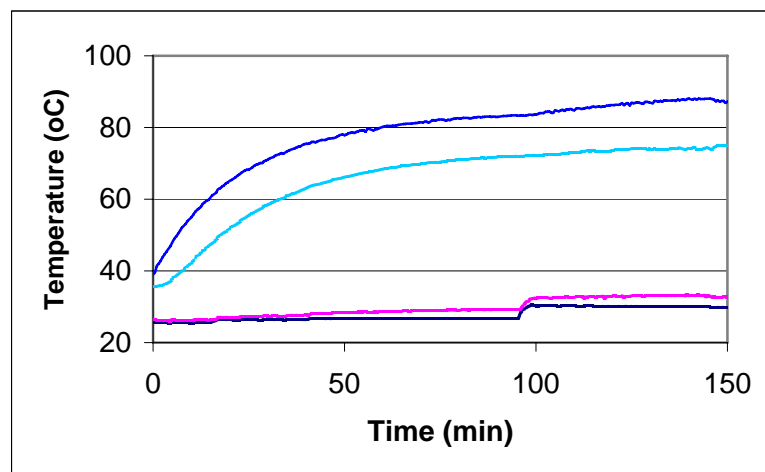


**Figure 6: Temperature response to startup from room temperature using  $F = 400$  cc/min**

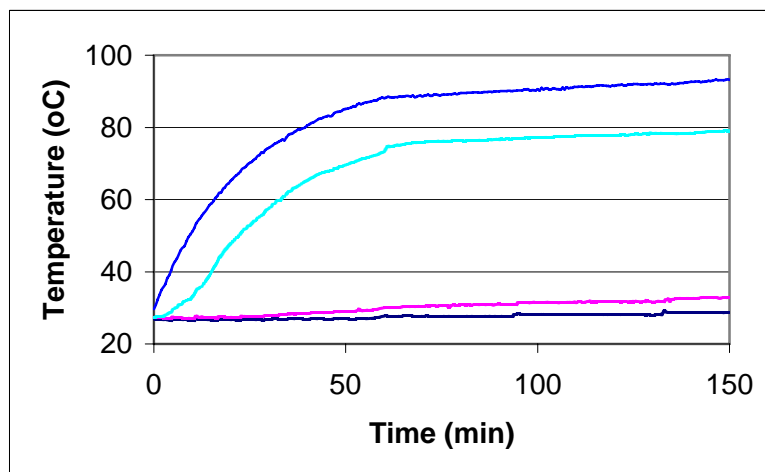


**Figure 7: Temperature response to startup from room temperature using  $F = 352$  cc/min**

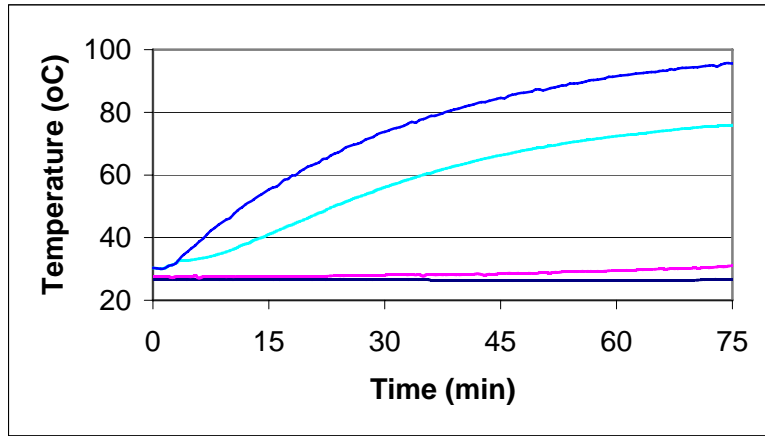


**Figure 8: Temperature response to startup from room temperature using  $F = 260$  cc/min**

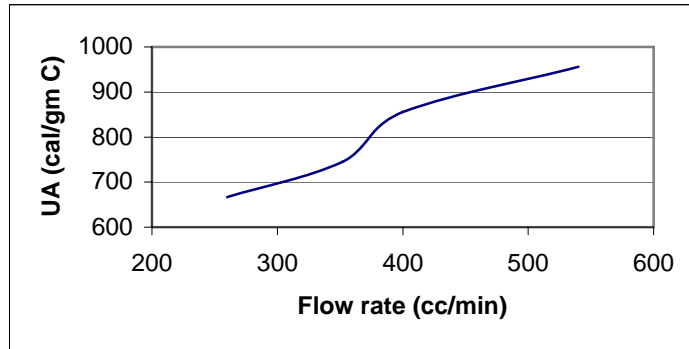


**Figure 9: The heater transfer coefficient versus the brine flow rate**

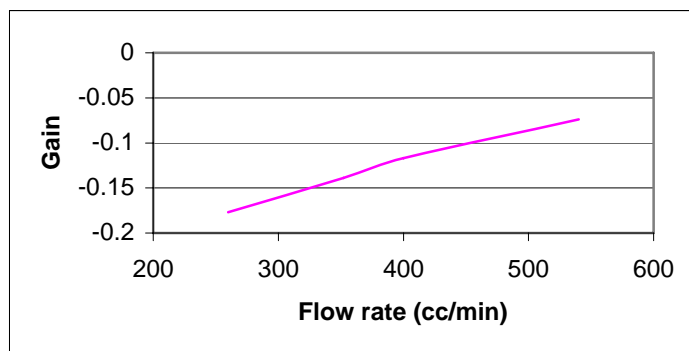


**Figure 9a: The process gain versus the brine flow rate**

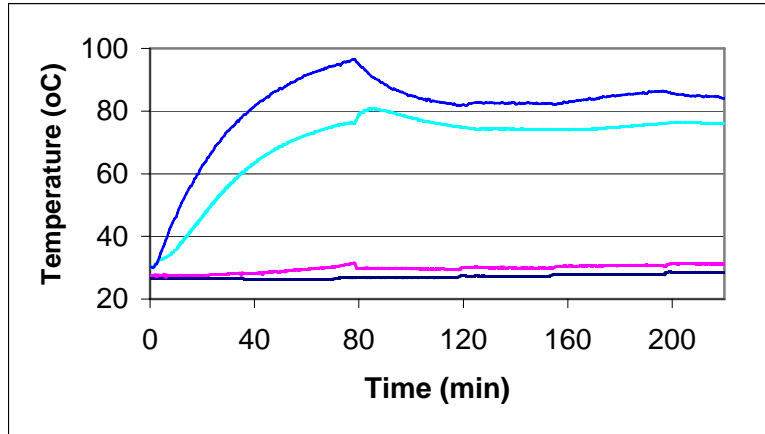


**Figure 10: Temperature response to two consecutive step changes in the brine flow rate**

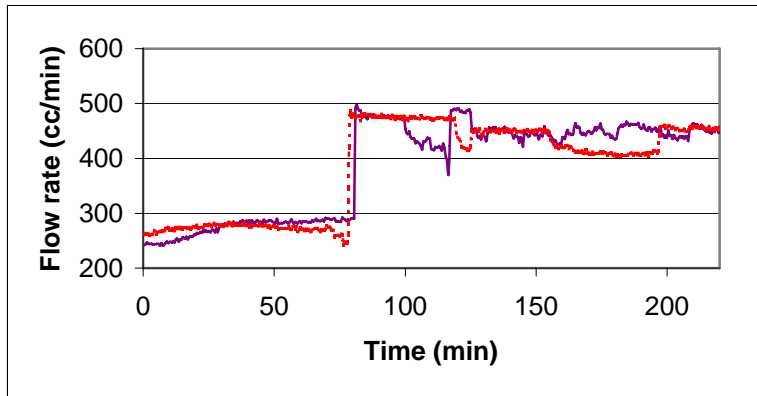


**Figure 10a: The brine flow rate for the step test in Figure 10; solid line: blow down, dashed line: circulating brine.**

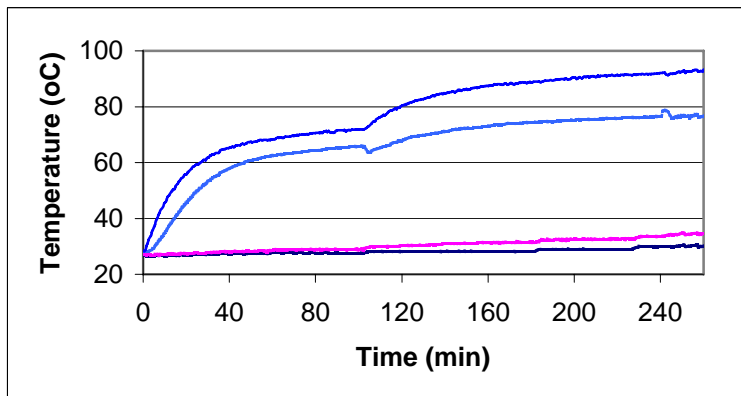


**Figure 11: Temperature response to two consecutive step changes in the brine flow rates**

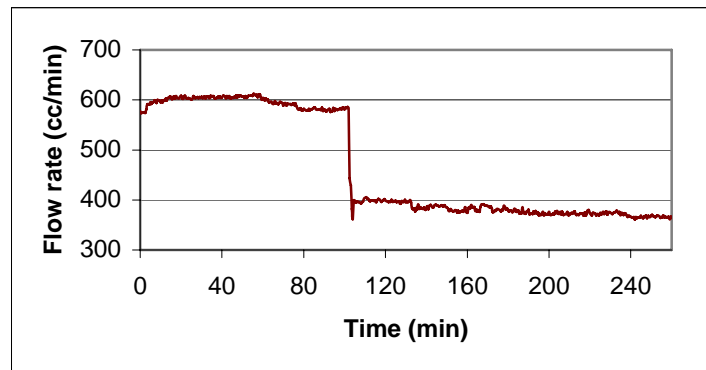


Figure 11a: The brine flow rate for the step test in Figure 11

### 8.1.2 Temperature startup at fixed pressure and brine flow:

The previous tests were carried out for fixed heat load and varying brine flow. In this section we examine the effect of varying the heat load at fixed brine flow. Similar to the previous case, the evaporator pressure will be fixed at atmospheric. In this case, the brine flow rate is fixed around 420 cc/min. The heat load will be varied by manipulating the heater power through a solid-state relay. The process is heated via two equal power electrical heater each of which delivers 1000 J/sec. One heater will be on continuously, while the other will be turned on/off periodically to simulate a certain percentage capacity. The percentage of the heater power capacity is discretized to span the capacity range of 0-100%. Each discretized percentage capacity is represented by a sequence of on/off signal scheme as shown in Table 2. The on/off signals are generated via the data acquisition system using a built-in module to produce a continuous square wave output. The high and low values as well as the duration of each phase, i.e. high/low, of the square wave can be adjusted by the user. However the hardware sets the minimum allowable duration of each phase equal to the sampling rate used. Therefore, to operate the heater at 25% of its capacity, the high/low values of the square wave are set to 5/0V, the duration of the high phase is set to one sampling time and the duration of the low phase is set to 3 sampling intervals.

Figures 12-17 demonstrates the temperature response to 0, 25, 50, 75, 90 and 100% power capacity for the electrical heater, respectively. The power capacity is set according to the procedure mentioned in the previous paragraph. This partial power

loading applies only on one of the heaters where the second one is fixed at maximum. The brine flow rate is fixed around 420 cc/min. Note that as shown in the figures the brine flow rate may fluctuate during operation because of many possible factors such as temperature changes, head pressure changes, air bubbles entrapment or impurities clogged in the flow transmitter. The blow-down flow is manipulated accordingly to maintain average brine level inside the evaporator. The non-smoothness of the temperature response shown in the figures especially for partial heat loading, i.e., 25-90%, is due to discretization of the power load. The response can be made smoother if smaller sampling time is used. As the figures demonstrate, the maximum attainable temperature for the heater and the brine increase with heat load. This is intuitive, but useful to evaluate the temperature gain with respect to heat load, which is essential for controller design. Also, the temperature responses can be used to determine proper operating conditions. For example, the temperature response with respect to different heat loads are plotted together in one graph (Figure 18). It should be noted that the temperature response for 90% loading reaches a steady state value less than that for 75% loading. This is because in the former case, the experiment was run at early morning time at which the inlet tank temperature is less than the other runs, which were carried out at afternoon time. Nevertheless, it is observed from Fig. 18 that the temperature responds nonlinearly to the heating load. Moreover, at heating load more than 75%, the process temperature has almost the same gain except that the time constant is slightly higher at 100% loading. If the process operation is chosen such that the brine flow is around 420 cc/min and the temperature around 80 °C, then the heater should operate at least at 75%. In this case, the process will operate close to its controllability region. This means that in case of minor disturbances, there is no sufficient heat load to reject the impact of the disturbance. Therefore, it is recommended to operate the process at lower brine flow, say 300 cc/min and 50% heat loading.

To examine the effect of changing heat capacity on the brine temperature, another test was conducted as shown in Figure 19a and 19b. The figures show the temperature start up operation starting from room temperature at fixed flow brine flow rate of 320 cc/min. The heat capacity was set at 100% for the first 90 minutes. Afterward, the heat capacity was stepped to 65% for the rest of the experiment. Due to the reduction in the heat load, the temperature reached a lower steady state value,

which is, as expected, indicates positive static gain. The sudden drop in the flash unit temperature is due to the fluctuation in the blow-down flow, which resulted in sudden drop of the brine level beyond the tip of the thermocouple submerged in the brine pool. By quick adjustment of the blow-down flow, the level is maintained and the temperature measurement is picked up correctly. Specifically, the brine temperature dropped about 4 °C in reaction to the 35% reduction in the heat capacity. This amounts to a static gain of 0.114 °C/% capacity.

Table 2: Discretization of power capacity of the heat load

| Power capacity in percentage | Total power capacity percentage | generator wave parameters, voltage signal at each sampling instant over 10 sampling instants |   |   |   |   |   |   |   |   |   |
|------------------------------|---------------------------------|--|---|---|---|---|---|---|---|---|---|
|                              |                                 | 0  | 0 | 0 | 0 | 0 | 0 | 0 | 0 | 0 | 0 |
| 0                            | 50                              | 0  | 0 | 0 | 0 | 0 | 0 | 0 | 0 | 0 | 0 |
| 10                           | 55                              | 5  | 0 | 0 | 0 | 0 | 0 | 0 | 0 | 0 | 0 |
| 20                           | 60                              | 5  | 0 | 0 | 0 | 0 | 5 | 0 | 0 | 0 | 0 |
| 30                           | 65                              | 5  | 5 | 5 | 0 | 0 | 0 | 0 | 0 | 0 | 0 |
| 40                           | 70                              | 5  | 5 | 5 | 5 | 0 | 0 | 0 | 0 | 0 | 0 |
| 50                           | 75                              | 5  | 0 | 5 | 0 | 5 | 0 | 5 | 0 | 5 | 0 |
| 60                           | 80                              | 5  | 5 | 5 | 5 | 5 | 5 | 0 | 0 | 0 | 0 |
| 70                           | 85                              | 5  | 5 | 5 | 5 | 5 | 5 | 5 | 0 | 0 | 0 |
| 80                           | 90                              | 5  | 5 | 5 | 5 | 5 | 5 | 5 | 5 | 0 | 0 |
| 90                           | 95                              | 5  | 5 | 5 | 5 | 5 | 5 | 5 | 5 | 5 | 0 |
| 100                          | 100                             | 5  | 5 | 5 | 5 | 5 | 5 | 5 | 5 | 5 | 5 |

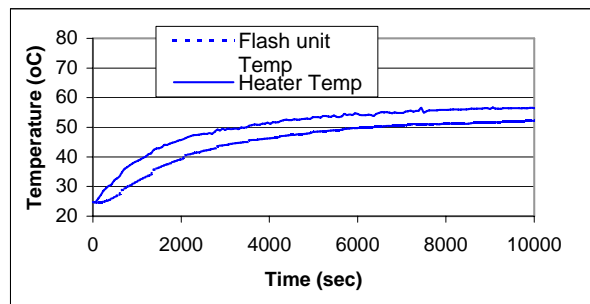


Figure 12a: Temperature response to 25% power capacity

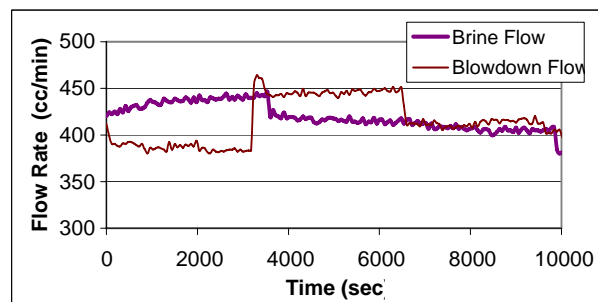


Figure 12b: Flow rate response for 25% power load

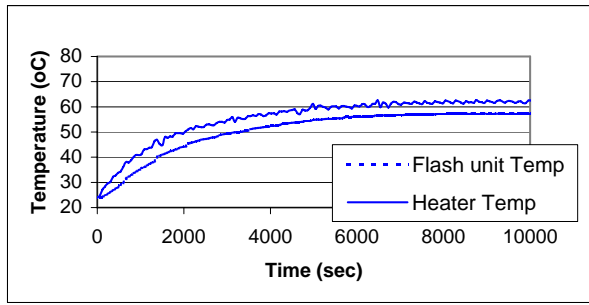


Figure 13a: Temperature response for 25% power capacity

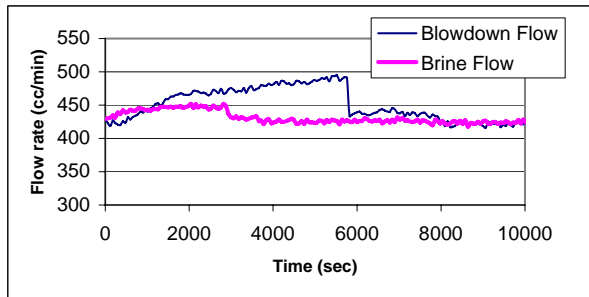


Figure 13b: Temperature response for 25% power capacity

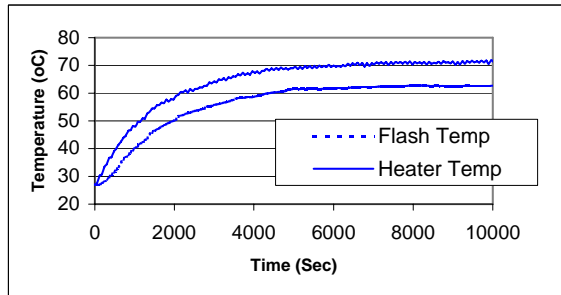


Figure 14a: Temperature response to 50% power capacity

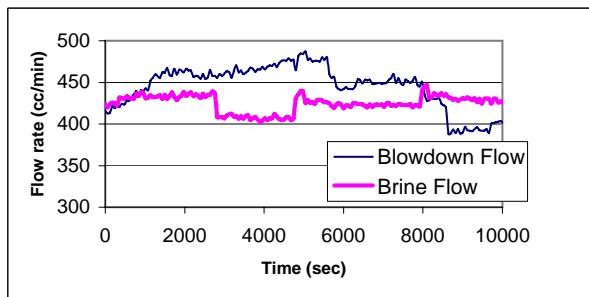


Figure 14a: Flow rate response for 50% power capacity

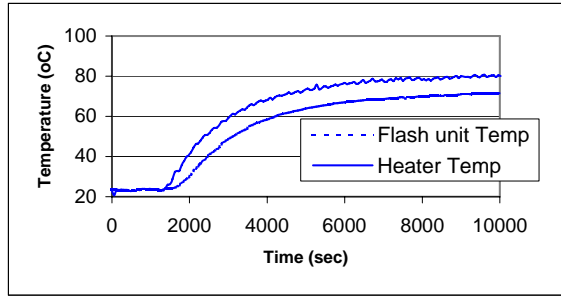


Figure 15a: Temperature response to 75% power capacity

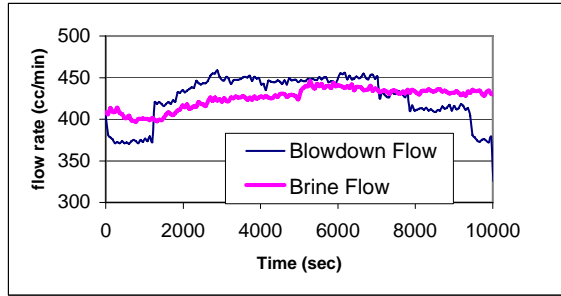


Figure 15b: Flow rate response for 75% power capacity

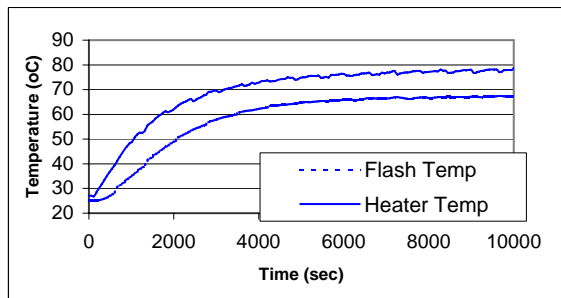


Figure 16a: Temperature response to 90% power capacity

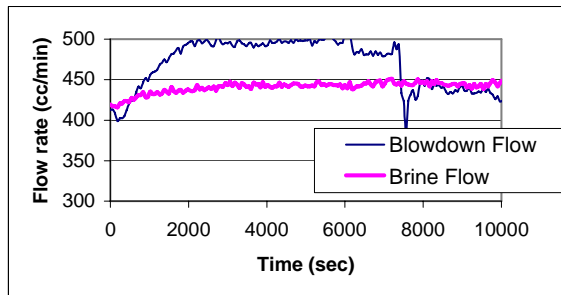


Figure 16b: Flow rate response for 90% power capacity

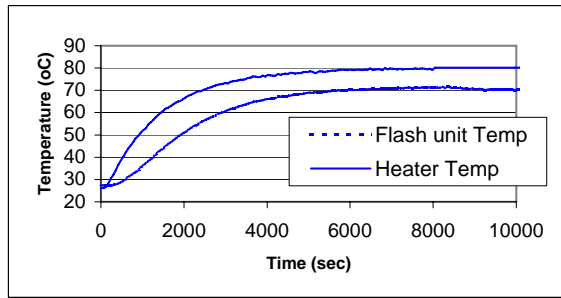


Figure 17a: Temperature response to 100% power capacity

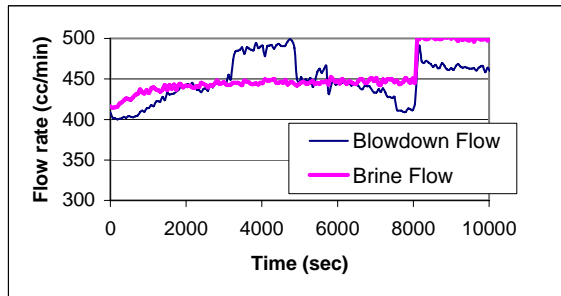


Figure 17b: Flow rate response for 100% power capacity

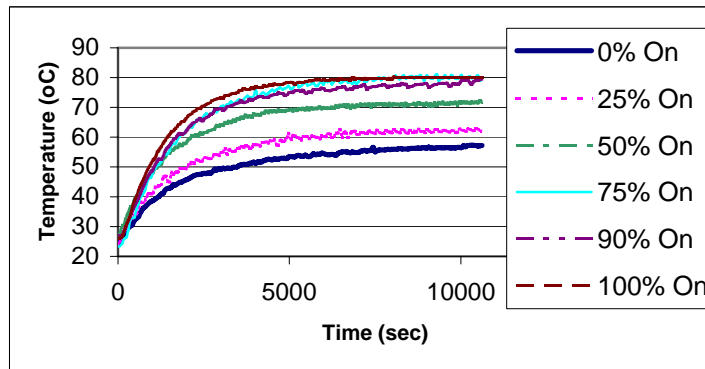


Figure 18: Temperature response to various power capacity

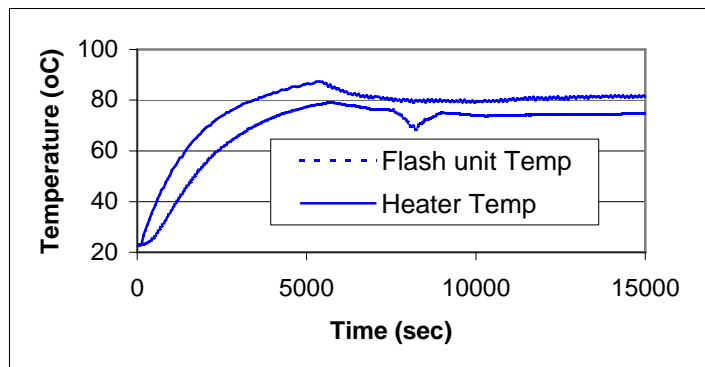


Figure 19a: Temperature response to two consecutive heat capacity operation

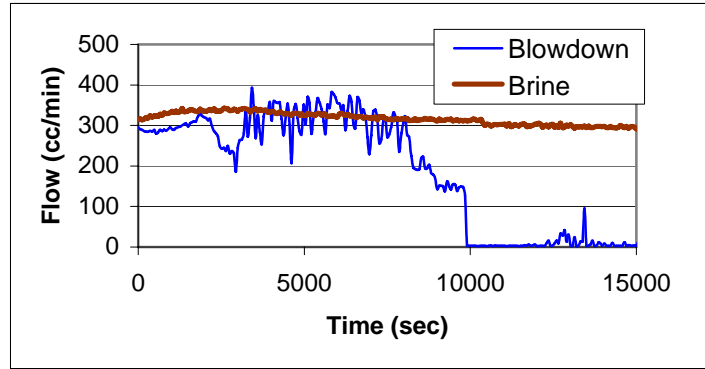


Figure 19b: Flow response to two consecutive heat capacity operation

The above open tests are repeated for other different values. The following table summarizes the main results at steady state.

Table 3: Steady state results for start up simulation at fixed heat load

| Fr<br>(cc/min) | $T_{Bi}$<br>(°C) | $T_{Bo}$<br>(°C) | T<br>(°C) | Q<br>(%capacity) | UA<br>(cal/min °C) | h<br>(cal/min °C) | Gain  | $\tau$<br>(min) |
|----------------|------------------|------------------|-----------|------------------|--------------------|-------------------|-------|-----------------|
| 560            | 30.3             | 68.6             | 72.4      | 100              | 1346.8             | 152.6             | 0.078 | 28              |
| 480            | 28               | 74               | 78.6      | 100              | 1151               | 143.1             | 0.102 | 34              |
| 400            | 32.7             | 77.5             | 85.4      | 100              | 759.1              | 178.15            | 0.131 | 34              |
| 320            | 32.3             | 81.3             | 91.8      | 100              | 555.1              | 194.61            | 0.176 | 34              |
| 240            | 32.3             | 81.3             | 96.1      | 100              | 350.7              | 237.97            | 0.235 | 40              |

Table 4: Steady state results for start up simulations at fixed brine flow rate

| Fr<br>(cc/min) | $T_{Bi}$<br>(°C) | $T_{Bo}$<br>(°C) | T<br>(°C) | Q<br>(%capacity) | UA<br>(cal/min °C) | h<br>(cal/min °C) | Gain  | $\tau$<br>(min) |
|----------------|------------------|------------------|-----------|------------------|--------------------|-------------------|-------|-----------------|
| 240            | 32.3             | 81.3             | 96.1      | 100              | 350.7              | 237.97            | 0.563 | 40              |
| 240            | 29.3             | 78.6             | 95.6      | 75               | 375.59             | 189.5             | 0.611 | 40              |
| 240            | 29.3             | 75.8             | 88.6      | 50               | 364.96             | 164.74            | 0.678 | 50              |
| 240            | 30.0             | 71.1             | 80.6      | 25               | 418.26             | 141.35            | 0.738 | 52              |
| 240            | 30.0             | 62.7             | 70.6      | 0                | 394.25             | 141.1             | 0.754 | 60              |

In the above table, the overall heat transfer coefficient for the brine heater tubes,  $UA$ , and the heat transfer coefficient for the air,  $h$ , the process gain and the time constant are calculated from the given experimental data at steady state. The gain for

the brine temperature with respect to brine flow rate is shown in Table 3, i.e. at constant heat load capacity of 100%, are calculated as the ratio of gained brine temperature to the brine flow rate. The gain for the other rows, i.e. at varying heat load capacity, the gain is taken as the ratio of the gained brine temperature to the heat capacity. The increase of the calculated gain with decrease in brine flow rate indicates negative process gain. This means that the top brine temperature decrease with increase in the brine flow rate. This is also obvious from the brine temperature shown in figures 10 and 11. The gain of the brine temperature with respect to the heat capacity is positive as shown in the table 4. The increase of brine temperature,  $T_B$ , with respect to  $Q$  is an indication of this positive gain. This obtained information regarding the static gain and time constant will be useful in designing the proportional-integral controller (PI) later in this report.

The calculated process unknown properties such as  $UA$  and  $h$  is also useful to understand the physical characteristics of this process. It is also useful for model validation. This will be utilized if advanced control is used for this unit. Anyway,  $UA$  is found to vary linearly with brine flow rate and can be approximated as follows:

$$UA = 1294 * F - 461.5$$

In table 2, the calculated values for  $UA$  vary although the feed flow rate is constant. The variation is attributed to measurement error and fluctuation in the brine flow. Moreover, the variation is small and centers on a mean value of 380. The heat transfer for the air,  $h$ , varies in table 3 and Table 4. Conceptually,  $h$  should not vary with the brine flow. However, the recorded trend for  $h$  shows that it increases with the heater temperature. This is in agreement with heat transfer fundamental because heat losses increases as the source temperature increases. Therefore, it makes more sense to correlate  $h$  with  $T$  as follows:

$$h = 3.5868 * T - 123.093$$

It can be noted that at higher brine flow, the heat transfer efficiency increases leading to small difference between the top brine temperature and the heated water temperature. Since the heat load is constant, the maximum steady state value for both

$T_{B0}$  and  $T$  is reduced. On the other hand, at lower brine flow rate, the heat transfer efficiency is reduced leading to smaller difference between the top brine temperature and the heated water temperature. Since the heat load is constant, the maximum steady state value for  $T$  is greater. According to Table 3 and 4, in order to operate the process at top brine temperature around 80 °C, the brine flow rate should be at least 320 cc/min. However, this requires operating the heater at maximum load. Therefore, there will be no room to reject the effect of disturbances. On the other hand, operating the process at low brine flow rate, will cause the heater temperature to reach high values, i.e. >95 °C, which is unsafe for the process equipment and accessories. Therefore, it is advisable to run the process at  $T_B = 75$  °C,  $B_r = 240$  cc/min, and  $Q = 50\%$  of its maximum value.

### **8.1.3 Startup up at fixed brine flow and heat load followed by flashing**

The previous open-loop tests were carried out at fixed pressure. No vacuum is introduced to produce distillate product. In this section, the process is started up from room temperature at fixed heat load of 50% for the second heater (equivalent to 65.2% overall) and fixed brine flow rate of 240 cc/min. This operating condition is determined by the analysis given in the earlier section. The result of the experimental run is shown in figure 20. As shown in the figure, the vacuum pump is tuned on when the brine temperature reaches 75 °C, which occurs two hours from the start of the experiment. The pressure inside the flash chamber reduces from 2.4 V (1 atm) to 1.6 V which is equivalent to 0.6 atm. As soon as the unit is vacuumed, the brine starts boiling. However, the vapor pressure reduces and consequently, the brine temperature drops. In addition, the vacuum operation increases the inlet brine flow rate. Since the flow and heat load is fixed, i.e. not regulated, the process stays at steady state with fixed evaporation rate. As shown in the figure, the brine temperature inside the condenser tube increases as more condensation occurs. The collected distillate over two hours of flashing operation is about 600 ml. This amounts to a distillate rate of 5 ml/min. To improve the flashing operation, regulation of the brine flow or the heat load should be considered.

## 8.2 Closed-loop runs

### 8.2.1 Temperature startup with on-off controlled brine flow

In the previous test, vacuuming increased the brine flow, which in turn reduced the steady state temperature. Here, the above test is repeated with the brine flow is maintained at its desired value through on/off control. The on-off controller regulate the valve opening for the brine stream to maintain its flow at desired value of 240 cc/min. The result of the experimental run is shown in Figure 21. The process is started from temperature using fixed heat load of 50% for the second heater. The vacuum is also controlled by manipulating a plead valve opening via on/off control scheme. The threshold for the vacuum controller is set at brine temperature of 75 °C. When the temperature is equal or higher than 75 °C, the vacuum valve is closed allowing the vacuum pump to suck the vapor out of the flashing chamber leading to higher vaporization rate. When the temperature is below 75 °C, the valve is opened allowing the flash chamber to breath leading to pressure build up. As shown in Figure 21, as the brine temperature reaches the threshold value, the pressure is reduced to 1,9 volt (corresponds to 0.8 atm) leading to increased vaporization rate. In this case, the brine temperature kept constant because the brine flow is maintained around its value through the on/off controller. Consequently, unlike the results in Figure 20, the brine temperature was kept steady because the flow is controlled. The collected distillate is about 600 mL over two hours of operation. The desalination rate is the same as that obtained in the earlier experiment.

### 8.2.2 Temperature startup with on-off controlled heater power

In the test, the process is started up from temperature using controlled heater power. One heater is on maximum power, while the other one is regulated using on-off scheme. The threshold value is set at 73 °C. The vacuum plead valve is also regulated via on-off scheme with threshold value of 74 °C. The result of this experimental run is shown in Figure 22. During the second hour of operation, the brine level inside the flashing chamber dropped below the tip of the thermocouple due to flow fluctuation. As a result erroneous reading for the brine temperature was observed. This in turn made the controller to keep heating the process leading to high heater temperature. With manual adjustment of the outlet brine flow, the brine level and consequently the temperature were stabilized. Figure 22 shows also the electrical

signal produced by the on-off controller and sent to the heater power source. In this case, 5 volts set the heater at maximum power and 0 volt turns the heater off. As shown by the figure reasonable control performance can be obtained using on-off scheme. The obtained distillate product over 2.5 hours of operations is 700 mL.

### 8.2.3 Temperature startup with PI controlled heater power

In this section, the process temperature is controlled during startup using PI control algorithm. In this case, the controlled output is the brine temperature and the manipulated variable is the heater power. The heater power is adjusted through regulating a solid-state (on-off) relay. To convert the on-off scheme into continuous function, a discretization approach similar to that shown in table 2 is used. The sampling rate for the controller law is 1 minute, this means that the PI control output is calculated each minute. However, the controller output is distributed over 5 sub-sampling intervals each of which span 12 seconds. For example if the PI controller output determine that the heater capacity should be set at 40% on, then the heater power is turned fully on for two consecutive sub-samples and off for the following three sub-samples. This sequence is equivalent to setting the heater off for 24 seconds and on for 36 seconds. Therefore, over an interval of one minute, the heater is set on for 40% of the time interval. The result of this experimental run is shown in figure 23. The PI controller gain is taken as  $k_c = 1.0$  and the integral time,  $\tau_i = 0$ . The set point for the brine temperature is 75 °C. The vacuum valve is also controlled via on-off scheme with threshold value of 74 °C.

As shown by Figure 23, the heater capacity was regulated at 100% in the beginning to startup the brine temperature from temperature. As the brine temperature reaches its set point, the PI controller starts regulate the heater power in order to maintain the brine temperature within its set point value. However, since no integral action is involved, the brine temperature offset by 2 degrees. The heater reaches a 40% capacity at steady state, however, some periodic spikes in the heater capacity are observed. The reason for these upsets is the measurement noise associated with the temperature readings. On the other hand, the vacuum valve was closed when the brine temperature reaches 73 °C for the first time, i.e. at time = 67 minute from the start of the experiment. However, the pressure is not reduced inside the flash chamber until

93 minutes have elapsed from the start of the experiment. This happened because the vacuum pump was off during that period. The collected amount of distillate is around 450 mL over two hours of vacuum operation. Less distillate rate is obtained because the brine temperature is 2 degree lower than its set point as mentioned earlier.

The performance of the closed-loop response can be further improved through better controller tuning. Generally, the Pi controller is tuned according to two well known methods. The following discusses these two techniques.

#### *Reaction curve tuning method*

The process dynamics can be represented by the response of a first-order system. This response can be represented mathematically by the following transfer function:

$$y(s) = \frac{k}{\tau s + 1} u(s)$$

Here,  $k$  is known as the static gain and  $\tau$  as the time constant. The static gain can be found from the above equation at steady state, i.e. at the limit as  $s$  goes zero:

$$y(\infty) = \lim_{s \rightarrow 0} y(s) = k\Delta a$$

Therefore,

$$k = \frac{y(\infty)}{\Delta a}$$

$y(\infty)$  is determined from the open-loop response of the process output to a step change.  $\Delta a$  is the step change in  $u$ . The time-domain solution of the above transfer function for step change is given as follows:

$$y(t) = k\Delta a(1 - e^{-t/\tau})$$

Note that at  $t = \tau$ , the last equation yields:

$$y(\tau) = 0.632k\Delta a = 0.632y(\infty)$$

This means that the response of  $y(t)$  reaches 63.2% of its final value when  $t = \tau$ . Therefore, the time constant can be estimated graphically which corresponds to the time instant at which the response is 63.2% complete. To determine the PI settings, the following regular formula [43] can be used:

$$k_c = \frac{\tau}{k}$$
$$\tau_I = \tau$$

#### *Continuous cycling tuning method*

The continuous cycling method is attributed to Ziegler and Nichols[44]. This classical approach is probably the best known method for tuning PID controllers. The continuous cycling method has also been referred as ultimate gain method. It is trial and error procedure, which can be summarized as follows:

*Step1:* Eliminate integral action by setting  $\tau_I$  at maximum and derivative action by setting  $\tau_D$  to minimum.

*Step2:* Set  $k_c$  at low value and the controller on automatic.

*Step3:* Increase the controller gain by small increments until sustained oscillation occurs after a small set point change.

The value of  $k_c$  that results in continuous cycling in Step 3 is referred to as the ultimate gain and will be denoted as  $k_u$ . The period of the resulting sustained oscillation is referred to as the ultimate period  $T_u$ . The PID controller settings are then calculated from  $k_u$  and  $T_u$  using the Ziegler-Nichols tuning relations. The Z-N tuning relations were empirically developed to provide 1/4 decay ratio. The Z-N relations are:

$$k_c = k_u/2.2$$

$$\tau_I = T_u/1.2$$

Note that the sampling rate and the sub-sampling rate affect the selection of the controller parameters, i.e.  $k_c$  and  $\tau_I$ . Therefore, to design the PI controller for this process, additional experiment runs are needed to determine the best values for the PI settings and the sampling rate.

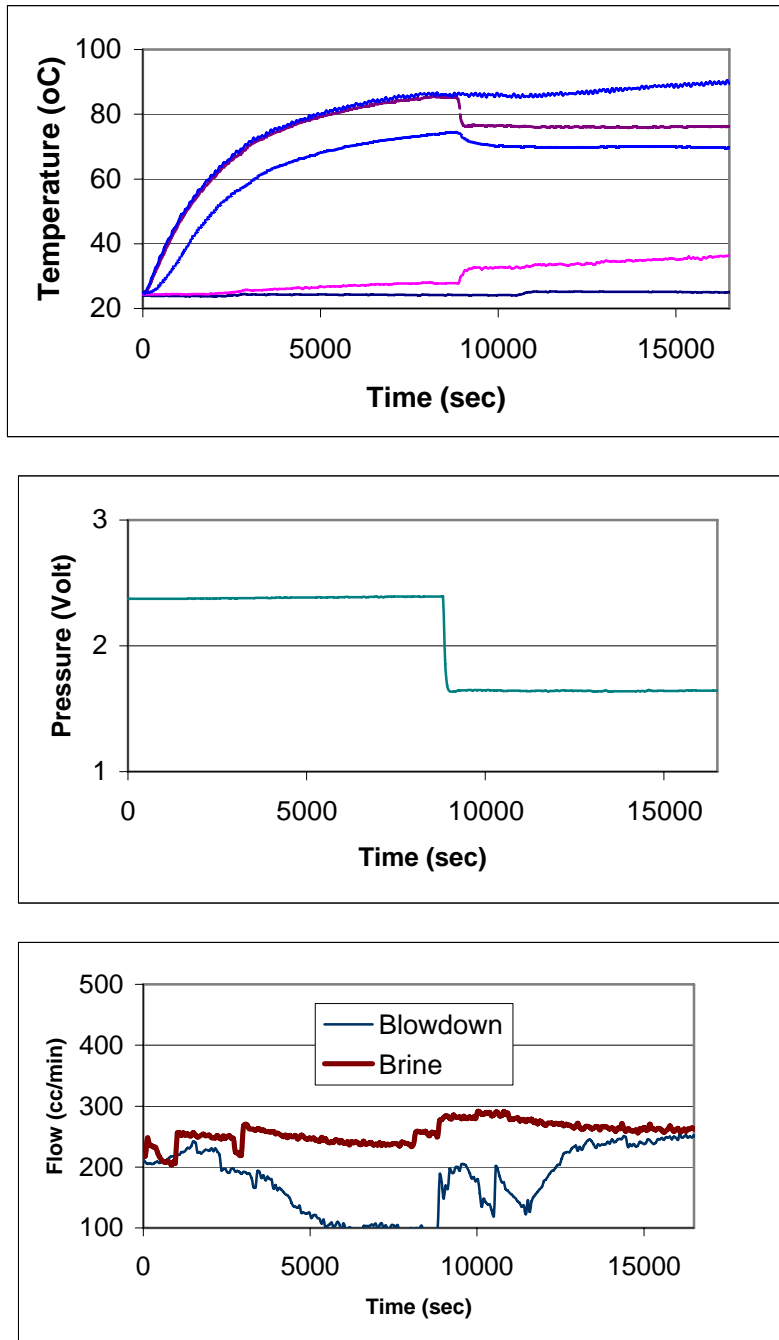


Figure 20: Open-loop response to flashing operation at fixed flow and heat load

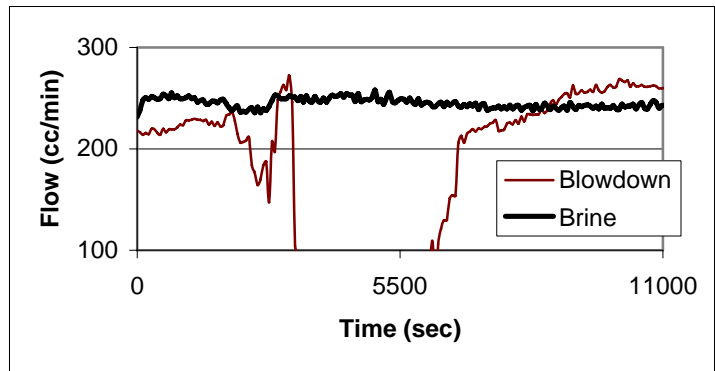
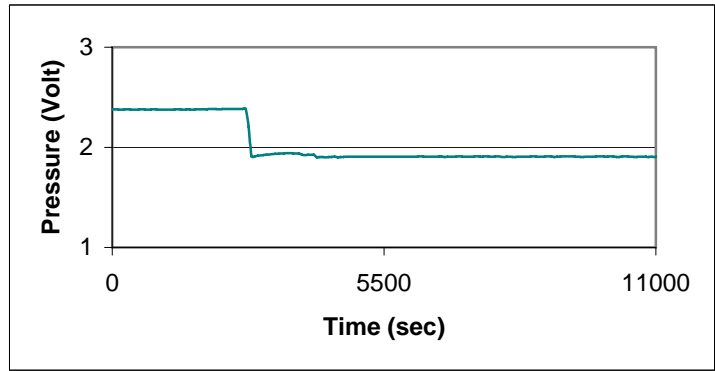
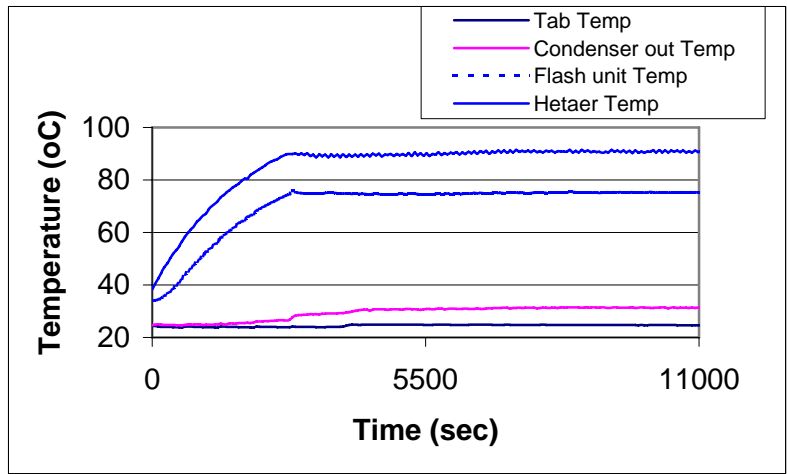


Figure 21: Temperature closed-loop response under vacuum

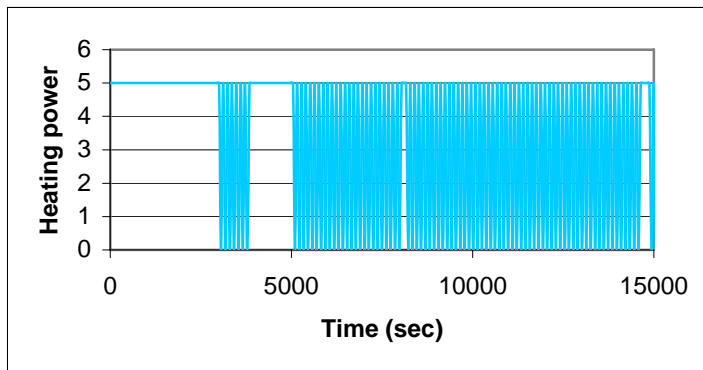
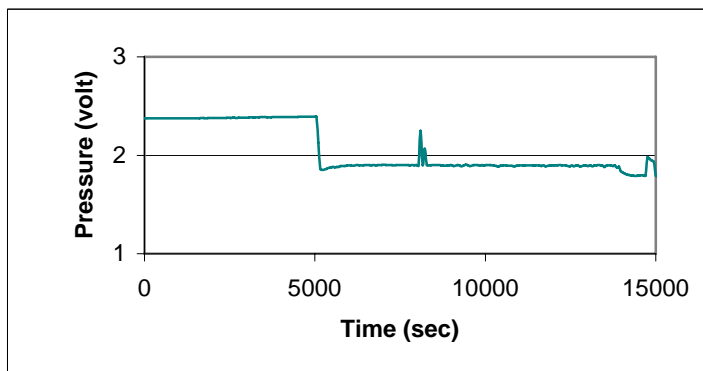
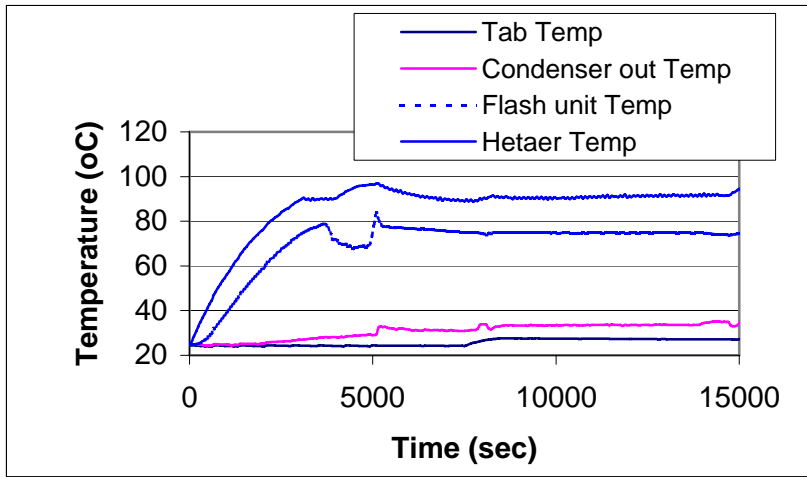


Figure 22: Temperature startup using on/off controlled heater

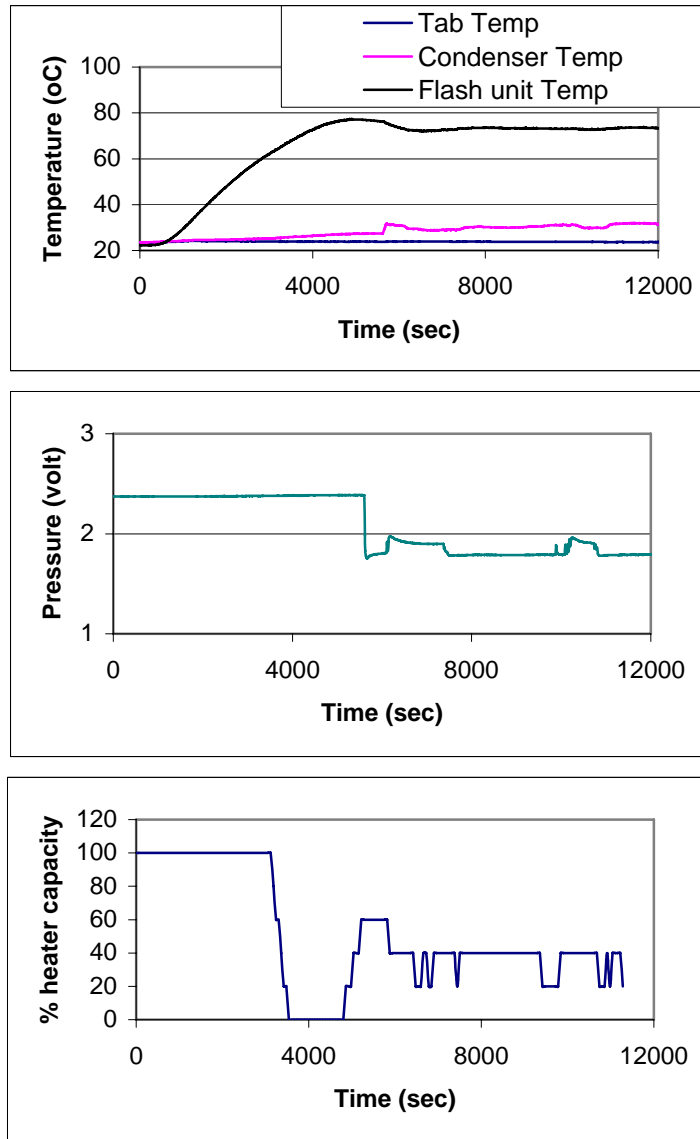


Figure 23: Temperature startup using Proportional controller

## Conclusions

An experimental setup for a single-stage flash desalination unit is designed and built. The unit is equipped with various digital sensors to record different states of the process. The sensors are connected to a PC computer through data acquisition system for data logging, storage and further analysis. The process and its accessories are calibrated and debugged. Several open-loop experimental operations were carried out to analyze the process dynamic and to identify some of its properties such as the overall heat transfer coefficient for the brine heater and the heat transfer coefficient for the air responsible for heat losses to the surrounding. The process is also tested for distillate production using vacuuming because the brine temperature is operated far below its normal boiling point. The normal boiling point is avoided for safety reasons and to avoid deterioration of the process equipment due to excessive heating. The distillate production improvement is investigated through simple control design.

Dynamic model for the process is also developed for given assumptions. The model is not validated with the experimental data. Intensive control design and analysis or application of advanced control is also not tested. The reason for not pursuing these objectives can be attributed to the following problems:

1. Shortage of time. In fact, most of the project time was consumed for equipment purchasing and installation. The absence of devoted or full-time lab technician delays the work progress substantially.
2. Failure or malfunctioning of some for the process equipment such as the Data acquisition system. Unfortunately, the failure of the DAQ system was not detected until the experiment was in the final phase for operation. By that time, the DAQ warranty was over worsening the situation. As a result, the DAQ has to be replaced.
3. The absence of research assistant to help in conducting some of the experimental runs.
4. Over-design of the process. The process has a long time constant. In fact, the experiment startup needs two hours to reach steady state. This means to conduct a meaningful experiment, 5-6 hours of operation is required, which is a lengthy time interval.

5. Technical problems such as:
- Fluctuation in the brine flow rate for unknown reasons, which makes handling the process very difficult.
  - Boiling in the brine heater. Water is used in the brine heater, which limits the highest achievable brine temperature especially at low flow rates.
  - Heat losses to the surrounding.
  - Limitation of the conductivity meters. The conductivity meters works at a maximum temperature of 40 °C. The blow-down operates at temperature much higher than 40 °C. A cooling path was designed for this purpose, however, the simplified design of the path was not enough to remove the considerable heat content.
  - Limitation of the data analysis software. The DAQ software, i.e. workbench, has a limited mathematical capability, which hinders the utilization of advanced control strategies.
  - Effect of vacuuming on the operation of the blow-down pump. Special type of pump is needed to stand the low pressure inside the flash chamber.

In order, to pursue the advanced project objectives, the above technical problems should be resolved. This may involve purchasing some hardware. In addition, more research time and assistants are needed. Nevertheless, the effort and the fund spent for this project is very rewarding as a complete well-running setup is obtained, which can be used to educate and train college students. Moreover, the gained knowledge and experience in designing, constructing and running the process is invaluable.

## Nomenclature

|           |  |
|-----------|--|
| $B_r$     | Brine mass flow rate, gm/min                                       |
| $B_D$     | Blow-down mass flow rate, gm/min                                   |
| $C_p$     | Heat capacity, cal/gm °C   |
| $h$       | Heat transfer coefficient for the air, cal/gm oC                   |
| $k$       | Process static gain  |
| $k_c$     | Pi controller gain   |
| $k^u$     | Ultimate gain  |
| $M$       | Mass holdup inside the flash chamber, gm                           |
| $MB$      | Mass holdup in the heated coil in the brine heater, gm             |
| $Mc$      | Mass holdup in the condenser tube, gm                              |
| $Q$       | Heat load, J/sec   |
| $T$       | Heated water temperature, °C                                       |
| $T_{ref}$ | Reference temperature, °C  |
| $T_a$     | Ambient temperature, °C  |
| $T_{Bi}$  | Brine temperature at heater inlet, °C                              |
| $T_{B0}$  | Brine temperature at heater outlet (top brine temp.), °C           |
| $T_{Bl}$  | Brine temperature at blow-down, °C                                 |
| $T_{ci}$  | Brine temperature at condenser inlet, °C                           |
| $T_c$     | Brine temperature at condenser outlet, °C                          |
| $T^u$     | Ultimate period  |
| $V$       | Water volume inside the heater, m <sup>3</sup>                     |
| $V_d$     | Vapor production rate, gm/min                                      |
| $UA$      | Overall heat transfer coefficient for the heater tubes, cal/min °C |
| $W_d$     | Distillate production rate, gm/min                                 |
| $X$       | Salt concentration, gm/gm water                                    |
| $X_i$     | Salt concentration at flash chamber inlet, gm/gm water             |
| $\rho$    | Water density, gm/l  |
| $\tau$    | Process time constant  |
| $\tau_I$  | Integral time  |
| $\lambda$ | Latent heat of vaporization, cal/gm                                |

## References

1. H. Ettouney, H. El-Dessouky and I. Alatiqi, "Understanding Thermal Desalination", *Chemical Engineering Progress*, September, 1999, 43-54.
2. K. Wangnick, "New IDA Worldwide Desalinating Plants Inventory," Report No. 15, *International Desalination and Water Reuse*, 8(2), Aug-Sep 1998, 11-12.
3. K. Wangnick, "Worldwide Desalinating Plants Inventory." Report No. 14, *International Desalination association (IDA)*, Topsfield, MA 1998.
4. E. Howe, "Fundamental of Water Desalination", Marcel Dekker, NY, 1974.
5. 'Desalination Technology 92' An intensive course, Porthan Ltd., 1992.
6. A. H. Khan, "Desalination Processes and Multistage Flash Distillation Practice", Elsevier Science Publisher B.V., 1986.
7. R. S. Silver, British Patent No. 829,819, September 1957.
8. R. S. Silver Engineering, London 1958, 25.
9. J. H. Beamer and Wilde, D. J., "The simulation and Optimization of a Single Effect MSF Desalination Plant", *Desalination*, 9, 1971, 259.
10. K. Hayakawa, Satori, H. and Konishi, K., "Process simulation on Multiflash Desalination Plant", *4<sup>th</sup> international Symposium on Fresh Water from Sea*, 1, 1973, 303.
11. M., Helal, Madni, M. S., Soliman, M. A., and Flower, J. R., "A TDM model for MSF Desalination Plants", *Comp. Chem. Eng.*, 10(4), 1986, 327-342.
12. S. Al-Mutaz, and Soliman, M. S., "Simulation of MSF Desalination Plants", *Desalination*, 74, 1989, 317.
13. A. R. Glueck, and Bradshaw, R. W., "A Mathematical Model for a MSF Desalination Plant", *3ed International Symposium on Fresh Water from the Sea*, 1, 1970, 95-108.
14. J. H. Delene, and Ball, S. J., "A Digital Computer Code for Simulating Large MSF Evaporator Desalinating Plant Dynamics", Oak Ridge National Laboratory, Report #ORNL-TM-2933, 1971.
15. M.A., Rimawi, Ettouney, H. M., and Aly, G. S. "Transient Model for MSF Desalination", *Desalination*, 74, 1989, 327-338.
16. K. V., Reddy, Hussain, A., Woldai, A., and Al-Gobaisi, D.M.K., "Dynamic modeling of the MSF Desalination Plant", Proceeding IDA world Congress on "Desalination and Water science", AbuDabi, 4, 1995, 227-242.

17. A. Hussain, Hassan, A., Al-Gobaisi, D. M. K., Al-Radif, A. Woldai, A., and Sommariva, C. *Arabian Gulf Regional Water Desalination Symposium*, Nov. 1992, 2 819.
18. A. Hussain, Woldai, A., Al-Radif, A., Kesou, A., Borsani, R., Sultan, H. and Deshpande, P. B., “Modelling and Simulation of a MSF Desalination Plant”, *Proceeding of the IDA and WRPC World Conference on Desalination and Water Treatment*, Nov. 1993, Japan, III, 119-159.
19. P.J. Thomas, S. Bhattacharyya, Patra, A., and Rao, G.P., “Steady State and Dynamic Simulation of Multistage Flash Desalination Plants: A case study”, *Comp. Chem. Eng.*, 22, 1998, 1515-1529.
20. A. Woldai, Al-Gobaisi, D.M.K, Johns, A.T, Dunn, R.W., and Rao, G.P. “Data Reconciliation for Control of MSF Desalination Processes”, *IDA*, 3, 1997, 181-188.
21. M. Bourouis, Pibouleau, L., Floquet, P., Domenech, S. and Al-Gobaisi, D.M.K, “Data Reconciliation and Gross Error Detection in Multistage Flash Desalination Plants”, *IDA*, 3, 1997, 167-180.
22. E. Ghiazza, Fumagalli, and Odicino, G., “The First Data Reconciliation and Optimization System for MSF Distillers Has Ben Installed on Al-Taweelah B”, *IDA*, 3, 1997, 79-90.
23. K. Al-Shayji, Liu, Y.A., “Neural Networks for Predictive Modeling and Optimization of Large Scale Commercial Water Desalination”, *IDA*, 3, 1997, 91-102.
24. M.E. ElHawary, “Artificial Neural Networks and Possible Application to Desalination”, *Proceeding of DESAL’ 92, Arabian Gulf E\Regional Water Desalination Symposium*, 15-17 November, 1992, UAE.
25. J. F. Olafsson, Jamshidi, M., and Titli, A., “On Fuzzy Control of Water Desalination Plants”, *LAAS Report 95197, LAAS-CNRS, Toulouse, France*, May 1995.
26. D. Barba, Liuzzo, G., and Tagliaferri, G., “Mathematical Model for Multi flash Desalinating Plant Control”, *4<sup>th</sup> International Symposium on Fresh Water from the Sea*, 1, 1973, 153.
27. Elsaie, M. H., Farrag M. F., and Efran, M. H., *Desalination*, 55, 1985 , 107.
28. D. M., Fareigh and Arazzini, S., *Desalination*, 55, 1985, 91.
29. H. Krause, and Hassan, A., “Optimization of MSF Plants as Integral Part of a Distributed Control system and as a Tool for Consultants”, *IDA*, 3, 1997, 151-166.

30. D. M. Al-Gobaisi, Hassan, A., Rao, G.P., Sattar, A., Woldai, A. and Borsani, R., "Towards Improved Automation for Desalination Processes Part I", *Advanced Control*, *Desalination*, 97, 1994, 469-506.
31. M.H.A. El-Saie, and Hafez, M.H.E., "Selecting and Tuning the Control Loops of Ms Desalination for Robustness", *Desalination*, 97, 1994, 529-540.
32. D. M. Al-Gobaisi, "A Quarter-Century of Seawater Desalination by Large Multistage Flash Plants in Abu Dhabi", *Desalination*, 1994.
33. A. Husain, Woldai, A., Al-Radhif, A., Kesou, A., Borsani, R., Sultan, H., and Deshpande, P.B., "Modeling and Simulation of a Multistage Flash (MSF) Desalination Plants", *Desalination*, 97, 1994, 555-586.
34. A. Ismail, "Control of Multistage Flash Desalination Plants: A Survey", *IDA*, 3, 1997, 21-38.
35. M.R. Akbarzadeh, and Kumbla, K.K., "Intelligent Control of Desalination Plants: GA-Fuzzy Approach", *International Symposium on Intelligent Automation and Control*, Montpellier, France, May 1996.
36. K.K. Kumbla, and Akbarzadeh, M.R., "intelligent Control of Desalination Plants: Neuro\_Fuzzy Approach", *International Symposium on Intelligent Automation and Control*, Montpellier, France, May 1996.
37. M.R. Akbarzadeh, Kumbla, K.K., Jamshidi, M. and Al-Gobaisi, D.M.K., "GA Optimization of PID Fuzzy Control of Desalination Plants", *IDA*, 3, 1997, 35-46.
38. A. Ismail, "Fuzzy Model Reference Learning Control of Multi-Stage Flash Desalination Plants", *IDA*, 3, 1997, 3-18.
39. V.M., Maniar and Deshpande, P.B., "Advanced Controls for Multistage Flash (MSF) Desalination Plant Optimization", *J. Process Control*, 6, 1996, 49-66.
40. Emad Ali, Abdelhamid Ajbar and Khalid Al-humaizi, "Robust Control of Industrial Multi Stage Flash Desalination Processes", *Desalination*, **114**, 1997, pp. 289-302..
41. Emad. Ali, Khilaid Alhumaizi, and Abdelhamid Ajbar, "Robust Control of Multi Stage Flash Desalination Plants Through Reduced Model", *Desalination*, **121**(1), 1999, pp. 49-64.
42. P.S. Sakar, Akbarzadeh, M.R., Jamshidi, T.M., and Al-Gobaisi, D.M.K., "Design and Modeling of a Laboratory Scale Single Stage Flash Desalination Plant", *IDA*, 3, 1997, 251-262.

43. Seborg, D., Edgar, T. and Mellichamp, D. *Process Dynamics and Control*. Wiley & Sons, 1989.
44. Ziegler, J. G., and N. B. Nichols, "Optimum Settings for Automatic Controllers", *Trans. ASME*, 64, 759, 1942.